Ontogenesis

Eco-evolutionary perspective on life history complexity

Hin, V.

Chapter 2

Evolution of Size-Dependent Intraspecific Competition Yields Paradoxical Predictions on the Scaling of Metabolism with Body Size

Vincent Hin

André M. de Roos

Manuscript in preparation

Abstract

Growth in body size is accompanied by changes in foraging capacity and metabolic costs, which lead to changes in competitive ability over ontogeny. The resulting size-dependent competitive asymmetry determines population and community dynamics, but it is not understood whether natural selection favors such asymmetry in intraspecific competition. We address this question using a size-structured consumer-resource model to study the evolution of the scaling of competitive ability with body size. Strength and direction of competitive asymmetry depend on the scaling exponents of maximum ingestion and maintenance metabolism with body size. We use adaptive dynamics to study evolution of these exponents and their dependence on mortality and life-history parameters. The two exponents converge to the same value, such that all individuals are competitively equal. Furthermore, the scaling exponents respond adaptively to changes in mortality such that growth and/or reproduction increases in the life stage that is affected most by mortality. Also, decreasing size at birth leads to increased investment in juvenile growth, while increasing maximum size leads to increased investment in post-maturation growth and reproduction. The latter result provides an explanation for the variation in intraspecific scaling exponents of metabolic rate with body size as observed in nature. Data will be presented that support these predictions. However, selection towards equal scaling exponents contradicts other empirical findings and explanations for this discrepancy will be discussed.

2.1 – Introduction

Intraspecific competition is often asymmetric such that some members of the population have a large negative effect on others, but suffer relatively little from competition themselves. Furthermore, this asymmetry most often depends on individual body size. For example, small larvae of the damselfly *Ischnuru elegans* suffer from reduced growth and longer developmental times due to interference of large larvae, but not from other small larvae (Gribbin and Thompson 1990). In case of competition for resources, or exploitative competition, the competitive ability of an individual is determined by resource foraging capacity and metabolic costs, which affect the ability to grow, reproduce and withstand resource scarcity (Hjelm and Persson 2001; Persson et al. 1998; Werner 1994). Foraging capacity has various behavioral and physiological components, such as attack rate, handling time, assimilation efficiency and resource supply rates. These processes generally scale with body size in different ways (Hansen et al. 1997; Persson et al. 1998; Peters 1983). The specifics of these scaling relationships determine whether large or small individuals are competitively superior. In fish, for example, the metabolic costs generally increase faster with body size than foraging capacity (Persson and De Roos 2006). Therefore, larger individuals need higher food quantities just to cover maintenance requirements and are therefore competitively inferior resource competitors compared to small individuals (Aljetlawi and Leonardsson 2002; Hjelm and Persson 2001; Kooijman 2010; Persson et al. 1998; Werner 1988). On the other hand, large individuals are likely to have more reserves and in combination with lower mass-specific maintenance requirements may hence withstand starvation better than small individuals (Byström et al. 2006).

Understanding intraspecific competitive asymmetry and its consequences for population and community dynamics from an individual perspective requires a measure that relates individual-level competitive performance to body size. Two such measures have been proposed previously: *i*) the mass-specific biomass production rate (MBP) (De Roos et al. 2013; De Roos and Persson 2013) and *ii*) the maintenance resource density (MRD; Persson et al. 1998), referred to by some authors as the critical resource density (Byström and Andersson 2005; Lefébure et al. 2014; Persson and De Roos 2006). The MBP describes the ability of an individual to produce new biomass through growth and reproduction with a certain amount of resources, expressed per unit body mass of the individual (De Roos et al. 2013). An individual with a high MBP can be considered competitively superior to one with a low MBP, since at the same resource level it can reproduce and grow with a higher mass-specific rate. The MRD is defined as the resource level at which an individual can just cover its maintenance metabolism, *i.e.* when the MBP becomes zero (Gliwicz 1990; Persson et al. 1998). The MRD can be interpreted as an individual-level R^*-value (sensu Tilman 1980), such that

competitively superior individuals have a lower MRD. Both the MBP and the MRD are derived from the difference between assimilation and metabolic maintenance costs. The scalings of the MBP and the MRD with body size can be used to determine whether small, intermediate sized or large individuals are competitively superior (Persson et al. 1998). However, the two measures do not necessarily have the same outcome. In the case of identical scalings of assimilation and maintenance rates, the MRD is a constant function of body mass, while the MBP can still increase or decrease with size when both these scalings are allometric (different from one).

Changes in the MBP and MRD with body size can have large consequences for population dynamics, species coexistence and community structure (reviewed in De Roos and Persson 2013; De Roos et al. 2003*a*; Persson and De Roos 2013). A change in the MBP with ontogeny implies that either large or small individuals produce more new biomass per unit of existing biomass and this causes a bottleneck in the flow of biomass across the life cycle. Such an energetic bottleneck considerably influences the population size distribution (De Roos et al. 2007), as biomass accumulates in the size-range with the lowest productivity. Increasing (size- or stage-specific) mortality can alleviate such a bottleneck and lead to an overcompensatory increase in biomass of the non-limited stage (De Roos et al. 2007). This phenomenon of biomass overcompensation is shown to occur in both experimental (Cameron and Benton 2004; Schröder et al. 2009*b*) and natural systems (Ohlberger et al. 2011) and can lead to community wide effects such as emergent Allee effects (De Roos et al. 2003*b*), emergent facilitation between two size-selective predators (De Roos et al. 2008*b*) and alternative stable states (De Roos and Persson 2002; Guill 2009; Schröder et al. 2014; Van Kooten et al. 2005).

The scaling of the MRD with body size has been used to explain the occurrence of population dynamic cycles (Persson et al. 1998). When the MRD changes over ontogeny some individuals have a negative energy balance and suffer from starvation, while others have a positive energy balance and can invest in growth and/or reproduction. This destabilizes population dynamics (De Roos and Persson 2003; Persson and De Roos 2013; Persson et al. 1998). An increasing MRD with body size leads to juvenile-driven cycles in which a single dominant cohort outcompetes all other individuals in the population. A decrease in the MRD with body size causes adult-driven cycles, which arise from a retardation of juvenile growth and hence an elongation of the juvenile period due to limited food availability. When the dominant cohort matures, this leads to a sudden increase in fecundity and adult biomass (De Roos and Persson 2003).

Besides its impact on population and community dynamics, asymmetric competition can considerably influence individual life history, with potential evolutionary consequences. For example, a modeling study on Trinidian guppies by Bassar et al.

(2016) revealed that the degree of asymmetry in competition changed both the mean and the variance of the generation time and life expectancy at birth and also the variance of the lifetime reproductive success. By changing the nature of the density-dependence, asymmetric competition is suggested to influence both the direction and speed of evolutionary life history changes (Bassar et al. 2016; Mylius and Diekmann 1995). However, explicit predictions about the eco-evolutionary dynamics of competitive asymmetry were not discussed by Bassar et al. (2016). Evolutionary consequences of intraspecific competition have mainly been studied in the light of ecological character displacement, where increased competition leads to diversification in diet and morphology between individuals (Bolnick 2004; Svanbäck and Bolnick 2007). It remains unclear how the degree and direction of asymmetry in competition affects eco-evolutionary dynamics and whether natural selection would lead to symmetric or asymmetric intraspecific competition.

Both the MBP and the MRD are derived from the energy budget of an individual and are controlled by the rates of assimilation and maintenance metabolism, which generally change allometrically with body size (Glazier 2005; Kleiber 1932; Kooijman 2010; Peters 1983; West et al. 2001). Allometric scaling relationships are described by power functions that contain a proportionality constant and a scaling exponent (Glazier 2005; Kleiber 1932; Peters 1983). Two competing frameworks model ontogenetic growth and provide a value for the allometric scaling exponents of assimilation and maintenance: the ontogenetic growth model of West, Brown and Enquist (OGM-model Hou et al. 2011, 2008; West et al. 2001; Zuo et al. 2012) and Dynamics Energy Budget (DEB) theory (Kooijman 2010; Maino et al. 2014; Sousa et al. 2008, 2010; Van der Meer 2006). In both models ontogenetic growth results from the difference between resource or energy supply and maintenance costs of existing cells (Kearney and White 2012; Van der Meer 2006; West et al. 2001). In the OGM-model energy supply is proportional to the resting metabolic rate, which is assumed to scale with three-quarters power of body mass (Hou et al. 2008; Savage et al. 2004; West et al. 2001). This three-quarters scaling follows from an independent model of a distribution network that delivers resources to terminal units (capillaries). Minimization of the energetic costs in such a network leads to a fractal-like distribution network in which the number of terminal units scales with three-quarters power to body mass (West 1997; West et al. 1999). DEB theory (Kooijman 2010) describes an individual in terms of structural body volume and reserve density. Resource supply is assumed proportional to structural surface area and hence scales with a two-thirds power of structural volume for isomorphically growing organisms, while maintenance costs increase isometrically with volume. This results in Von Bertalanffy growth curves (Kooijman 1986, 2010). As Ricklefs (2003) points out, the two growth models are specific versions of

a broader class of ontogenetic growth models and discriminating between the two on the basis on growth data is often impossible (Banavar et al. 2002).

Recently, data is accumulating that indicates substantial variation in the value of the scaling exponent of metabolic rate and this variation has been related to taxonomic diversity, lifestyle in aquatic organisms (pelagic vs. non-pelagic), temperature, life stage, activity level, physiological state, predation and body shape (Burton et al. 2011; Caruso et al. 2010; Glazier 2005, 2006, 2009; Glazier et al. 2011, 2015; Hirst et al. 2014; Killen et al. 2010). Glazier (2005) argues that the diverse scaling relationships observed in nature result from diverse adaptations in combination with ecological physico-chemical constraints. This suggests that scaling exponents can change adaptively, for example through changes in body shape during ontogeny (Hirst et al. 2014; Killen et al. 2010; Ohlberger et al. 2011). Such changes would alter the degree of competitive asymmetry within the population and have substantial consequences for population and community dynamics, as well as individual life history. However, explicit predictions about the evolutionary dynamics of competitive asymmetry are missing. Therefore, the main purpose of this study is to understand the selection pressures that act on the scaling of competitive ability with body size.

We formulate an individual-level, dynamic energy budget model that describes ingestion, maintenance, growth and reproduction as a function of body mass and resource density. Both assimilation and maintenance rates follow power functions of body mass. The individual-level model is translated to a population-level model by considering the density distribution of individuals along the body mass axis, as in the framework of physiologically structured population models (De Roos 1997; De Roos and Persson 2001; Metz and Diekmann 1986). We explore how the scaling exponents of assimilation and maintenance affect population dynamics and subsequently study the evolutionary dynamics that result from selection pressures on these scaling exponents. Fitness and the direction and strength of selection arise through the feedback between an individual and its environment (Metz et al. 1992). Therefore, we use the framework of adaptive dynamics to study evolutionary change and identify evolutionary endpoints of the scaling exponents of maximum ingestion and maintenance rates (Durinx et al. 2008; Geritz et al. 1998; Metz 2012; Metz et al. 1992).

2.2 – Model description

Ecological dynamics

A dynamic energy budget (DEB) model specifies the rates of resource ingestion, maintenance, growth, reproduction and mortality of an individual, as a function of its body size and resource density. All equations of this model are shown in table 2.1. Both growth and reproduction are modeled as food-dependent processes. The competition for food is incorporated explicitly by considering a dynamic resource on which all consumer individuals feed. A net-production energy budget model is used to model the allocation of resources to the processes of maintenance, growth and reproduction (Gurney and Nisbet 1998; Lika and Nisbet 2000). In a net-production model, maintenance always takes precedence over growth or reproduction. Hence, reproduction and growth are impossible when food conditions are insufficient to cover maintenance requirements. Both maximum ingestion rate and maintenance rate are power functions of body mass. For an individual with mass s the maximum ingestion is given by $M(\frac{s}{s_r})^Q$ and maintenance rate by $T(\frac{s}{s_r})^P$. Here, M and T are, respectively, the maximum ingestion rate and maintenance rate of an individual with body mass s_r. The exponents Q and P describe how these rates scale with body mass s. An increase in Q and P implies an increase in, respectively, the maintenance rate and maximum ingestion rate for individuals with $s > s_r$ and a decrease for individuals with $s < s_r$. Individuals are born with size s_b, mature at size s_j and can reach a maximum size of s_m, when food density is sufficient. In case $s_b < s_r < s_m$ there is a trade-off between individuals with $s < s_r$ and conspecifics with $s > s_r$, for both maximum ingestion rate and maintenance rate. By default a juvenile-adult trade-off is assumed by setting $s_r = s_j$, but deviations from this assumption are explored. Besides the size-dependent maximum ingestion rate, the rate of food ingestion, $I(R, s)$, follows a Holling type-II functional response of resource biomass R with a size-independent half-saturation constant H (see table 2.1). Ingested food is assimilated with efficiency σ and maintenance costs are subtracted from assimilated biomass (Lika and Nisbet 2000). We assume that the conversion efficiency σ includes all the overhead costs involved in producing new biomass through somatic growth or reproduction. The production rate of biomass, denoted by $\Omega(R, s)$, is hence equal to the assimilated biomass minus the maintenance costs (table 2.1).

Depending on the scaling exponents of maintenance and maximum ingestion, individuals can grow to very large body sizes. To prevent this, we model adult allocation towards growth by an sigmoid function $\kappa(s)$ that decreases from one at maturation size s_j towards zero at the maximum individual body size s_m (table 2.1). Hence, asymptotic size is limited to s_m when food availability is sufficient, but this size might not be reached when food is limited. The production not spent on growth

Table 2.1 – Model Equations

Equation	Description
$I(R, s) = M \left(\frac{s}{s_r}\right)^Q \frac{R}{R+H}$	Resource ingestion
$\Omega(R, s) = \sigma I(R, s) - T \left(\frac{s}{s_r}\right)^P$	Biomass production
$\frac{ds(R, a)}{da} = g(R, s) = \kappa(s)\Omega^+(R, s)$ with $s(R, 0) = s_b$	Growth rate
$b(R, s) = \frac{(1-\kappa(s))\,\Omega^+(R, s)}{s_b}$	Fecundity rate
$\kappa(s) = \begin{cases} 1 & \text{for } s < s_j \\ 1 - 3L(s)^2 + 2L(s)^3 & \text{for } s_j \le s < s_m \\ 0 & \text{for } s = s_m \end{cases}$ with $L(s) = \frac{s-s_j}{s_m-s_j}$	Allocation function
$\mu(R, s) = \begin{cases} \mu_c + \mu_j - \frac{\Omega^-(R,s)}{s} & \text{for } s < s_j \\ \mu_c + \mu_a - \frac{\Omega^-(R,s)}{s} & \text{for } s \ge s_j \end{cases}$	Mortality rate
$G(R) = \delta\,(R_{max} - R)$	Resource growth rate

We use $\Omega^+(R, s)$ to denote $\max(\Omega(R, s), 0)$ and $\Omega^-(R, s)$ means $\min(\Omega(R, s), 0)$

is allocated to reproduction in adults, whereas juveniles ($s_b \le s < s_j$) are assumed to spend all production of biomass on growth.

Growth in mass with age a occurs only when the biomass production rate, $\Omega(R, s)$, is positive and is given by the differential equation $\frac{ds(R,a)}{da}$ in table 2.1, with the size at birth as initial condition. Similarly, reproduction only occurs for positive values of $\Omega(R, s)$ and individual fecundity (the rate of offspring production per adult) is given by the function $b(R, s)$ (see table 2.1). Mortality is represented by the function $\mu(R, s)$ which is composed of background mortality μ_c for all individuals and additional size-dependent mortality for juveniles, μ_j, and adults, μ_a (table 2.1). Furthermore, mortality increases when food conditions are insufficient to cover maintenance requirements. This starvation mortality is equal to the magnitude of the mass-specific biomass production when negative. Starvation is handled as an increase in mortality instead of a reduction in body mass. Resource growth follows semi-chemostat dynam-

ics given by the function $G(R)$, with turn-over rate δ and maximum resource density R_{max} (table 2.1).

Model equilibria were computed using the software package PSPManalysis, which is especially designed for demographic, equilibrium and evolutionary analysis of physiologically structured population models (De Roos 2016). The basic method of PSPManalysis involves the numerical integration of a set of coupled ordinary differential equations that describe the change over age a of four life-history characteristics: growth, survival, cumulative resource ingestion and cumulative reproduction. This system of ODEs is integrated repeatedly, while iteratively adjusting the value of the equilibrium resource density $\tilde{R}$ until a solution has been found that satisfies the equilibrium condition. This equilibrium condition is given by the equation $R_0 = 1$, where R_0 represents the lifetime reproductive success of a single individual, given by:

$$R_0 = \int_0^\infty b(\tilde{R}, s(\tilde{R}, a))F(\tilde{R}, a)da \tag{2.1}$$

Here, $b(\tilde{R}, s)$ is the fecundity at equilibrium and the expression $F(\tilde{R}, a)$ is the survival function at equilibrium, which follows from:

$$F(R, a) = e^{-\int_0^a \mu(R, s(R,\alpha))d\alpha} \tag{2.2}$$

Subsequently, the population-level birth rate in equilibrium, $\tilde{B}$, is calculated from the condition that in equilibrium the resource growth rate should equal total population-level foraging:

$$\delta(R_{max} - \tilde{R}) = \tilde{B}\int_0^\infty I(\tilde{R}, s(\tilde{R}, a))F(\tilde{R}, a)da \tag{2.3}$$

The integrals in equations 2.1, 2.2 and 2.3 are calculated by the PSPManalysis package through numerical integration of the ODEs for cumulative reproduction, survival and cumulative resource ingestion, respectively. With the equilibrium values for the resource density, $\tilde{R}$, and population-level birth rate, $\tilde{B}$, the consumer size distribution follows from (De Roos 1997):

$$\tilde{m}(s) = \frac{\tilde{B}}{g(\tilde{R}, s)}\exp\left(-\int_{s_b}^{s}\frac{\mu(\tilde{R}, \xi)}{g(\tilde{R}, \xi)}d\xi\right) \tag{2.4}$$

Using 2.4 juvenile (J) and adult (A) biomass are given by the integral over the size distribution, weighted with body mass s:

$$J = \int_{s_b}^{s_j} s\tilde{m}(s)ds \tag{2.5a}$$

$$A = \int_{s_j}^{s_m} s\tilde{m}(s)ds \tag{2.5b}$$

The PSPManalysis package calculates model equilibria and stage-specific biomass densities (eqs. 2.5a and 2.5b) as a function of any model parameter by means of numerical curve continuation as described in Kirkilionis et al. (2001), Diekmann et al. (2003) and De Roos et al. (2010). The equilibrium analysis was complemented by numerical studies of transient and non-equilibrium dynamics of the model using the Escalator Boxcar Train (EBT) method (De Roos 1988; De Roos et al. 1992). The EBT method calculates population dynamics as a function of time by dividing the size distribution into cohorts of similarly-sized individuals and for every timestep calculating the growth, mortality and reproduction for each cohort, as a function of the body mass of individuals within that cohort and resource density.

Evolutionary dynamics

To study evolutionary dynamics we use the framework of adaptive dynamics, which assumes timescale seperation between ecological and evolutionary dynamics and that evolution is mutation limited (Durinx et al. 2008; Geritz et al. 1998; Metz 2012; Metz et al. 1995). Evolution then boils down to a series of trait substitutions that can result in an evolutionary singular strategy (ESS). At such an ESS, the selection gradient becomes zero and the population either resides at a (local) fitness maximum (evolutionarily stable) or when at a local fitness minimum, undergoes evolutionary branching due to disruptive selection (Doebeli and Dieckmann 2000; Geritz et al. 1998). Since our model has a one-dimensional environment, the occurence of evolutionary branching is impossible and all the ESSs that we encounter are convergence and evolutionarily stable (continuously stable strategies; Eshel 1983). For the selection gradient we use the derivative of lifetime reproductive success with respect to a particular trait p (*i.e.* model parameter) that is subject to evolution. In our model, an ESS obeys the conditions $\frac{\partial R_0(\tilde{R},p)}{\partial p} = 0$. When calculating the model equilbria as a function of trait values, the PSPManalysis software package automatically detects and classifies evolutionary singular strategies according to the subdivision presented in Geritz et al. (1998). Furthermore, the PSPManalysis package is used to calculate evolutionary isoclines. Such a line shows the value of an ESS of one trait (the evolutionary parameter), as a function of a second trait (Dieckmann 2002). We calculating both the evolutionary isocline of Q as a function of P, and vice versa, the evolutionary isocline of P as a function of Q. The intersecting of these two isoclines is the CSS of both Q and P.

Model parameters

The parameters and their default values are summarized in table 2.2 and a more detailed description of the parameter derivation is given in De Roos and Persson (2013). Body size of the consumer is expressed in grams (g) and biomass densities

Table 2.2 – Model Parameters

Symbol	Unit	Value	Description
R_{max}	$mg\ L^{-1}$	30	Maximum resource density
δ	day^{-1}	0.01	Resource renewal rate
Q	–	1	Maximum ingestion exponent
P	–	1	Maintenance exponent
M	$g\ day^{-1}$	0.1	Maximum ingestion constant
T	$g\ day^{-1}$	0.01	Maintenance constant
μ_c	day^{-1}	0.0015	Background mortality
μ_j	day^{-1}	0.0	Additional juvenile mortality
μ_a	day^{-1}	0.0	Additional adult mortality
σ	–	0.5	Assimilation efficiency
H	$mg\ L^{-1}$	3	Half-saturation density
s_b	g	0.1	Size at birth
s_j	g	1	Size at maturation
s_r	g	1	Scaling reference size
s_m	g	10	Maximum size

are expressed in milligrams per liter ($mg\ L^{-1}$). Across differently-sized species, the mass-specific maximum ingestion, mass-specific maintenance and mortality rates are inversely proportional to the quarter power of adult body size (Kleiber 1932; Peters 1983; Savage et al. 2004). Taking time in days and adult body weight in grams, representative proportionality constants of these scaling relationships for invertebrate species are 0.1, 0.01 and 0.0015 for maximum ingestion, maintenance and mortality, respectively (De Roos and Persson 2013). For the parameterization we take the characteristic adult body mass to equal the size at maturation, for which we adopt a value of 1 gram. Hence $M = 0.1$, $T = 0.01$ and $\mu_c = 0.0015$. A value of 0.01 is adopted for the resource renewal rate δ, so that resource turn-over equals the mass-specifc maintenance rate of an individual with size s_j. Only a change in the ratios between these four rates changes model predictions, as changing their absolute values all with the same factor only scales the unit of time. Values for the volume related parameters are $R_{max} = 30\ mg\ L^{-1}$ and $H = 3\ mg\ L^{-1}$ (table 2.2). The value for H is derived from zooplankton grazing rates as presented by Hansen et al. (1997) and R_{max} is assumed one order of magnitude larger than H (De Roos and Persson 2013). As long as the ratio of these volume-related parameters remains constant a change in these parameters

is equivalent to a scaling of the volume in which the consumer-resource interaction takes place. This does not qualitatively change model predictions. Default parameters for size at birth and maximum size are 0.1 and 10, but these values are changed during model analysis. The scaling exponents Q and P are varied throughout the analysis, but their values are limited to the range 0.4–1.3, which is the observed range of intraspecific scaling exponents found by Clarke and Johnston (1999) for post-larval teleost fish.

2.3 – Results

Measures of competitive asymmetry

One measure for competitive ability is the mass-specific biomass production (MBP) rate. For the same resource densities individuals with a higher MBP can be considered competitively superior. According to this measure, size-independent competition only occurs when the MBP is a constant function of body mass s:

$$\frac{d}{ds}\left(\frac{\Omega(R,s)}{s}\right) = 0. \tag{2.6}$$

From the expression for $\Omega(R, s)$ in table 2.1, it can be inferred that this only holds when $Q = P = 1$.

Another measure of competitive ability is the maintenance resource density (MRD), which is the resource level at which the MBP equals zero and follows from solving $\Omega(R, s) = 0$ for R:

$$MRD = \frac{T\left(\frac{s}{s_r}\right)^P H}{\sigma M\left(\frac{s}{s_r}\right)^Q - T\left(\frac{s}{s_r}\right)^P} \tag{2.7}$$

Individuals with a lower MRD are competitively superior to those with a higher MRD. It can be easily seen from equation 2.7 that the MRD is a constant function of body mass s when $Q = P$, irrespective of the value of Q and P. Hence, under the measure of the MRD competition is symmetric when $Q = P$, while under the measure of the MBP competition is symmetric when $Q = P = 1$.

Equilibrium and evolutionary analysis of Q and P

Exploring the model equilibria as a function of Q and P shows a similar pattern. In case $P > Q$, the maintenance rate increases faster with body mass s than the maximum ingestion rate (low Q values at left-hand side in figure 2.1A-D, high P values at right-hand side in figure 2.1E-H). Consequently, the MBP decreases with size while the MRD increases with body size. In such a population, the smallest individuals are most competitive and competitive ability decreases with size. A stable equilibrium results

in which the asymptotic body size is well below the maximum possible asymptotic size (figure 2.1D,H), due to the low competitive ability of adults. Adults grow until they spend all their assimilated biomass on maintenance and cannot grow any further. This explains the coincidence of the equilibrium resource density with the MRD of the largest individuals in the population for $Q < P$ (figure 2.1A,E). Because of the low competitive ability of adults, total productivity in the adult stage is insufficient to compensate for adult biomass loss due to mortality. This results in a net biomass loss in the adult stage, which is compensated for by a net biomass gain in the juvenile stage. This is shown by the fact that the total rate of biomass recruitment to the adult stage through maturation, is larger than the total rate of biomass recruitment to the juvenile stage through reproduction (figure 2.1C,G). Juveniles therefore grow rapidly, but growth and reproduction of adult individuals is slow since they spend a considerable amount of their assimilated biomass on maintenance. As a result total population biomass mainly consists of adult individuals (figure 2.1B,F).

When the maximum ingestion rate increases faster with body size than the maintenance rate, the MBP increases with body size, while the MRD decreases with body size. This means that large individuals are competitively superior ($Q > P$; large Q values at right-hand side in figure 2.1A-D, small P values at left-hand side in figure 2.1E-H). This results in adult-driven cycles in which adults that are close to the maximum size (figure 2.1D,H) hinder growth of the newborn cohorts. Growth of newborns only occurs when background mortality has sufficiently diminished adult density to allow the resource density to increase above the MRD of newborn individuals (figure 2.1A,E). Because individuals increase in competitive ability during growth, the growing juveniles decrease resource density again and inhibit growth of later cohorts. If abundant enough, these later cohorts will either catch up with the earlier produced individuals when resource densities increase again, or die due to background and starvation mortality. Adult-driven cycles exists for $P = 1$ and $Q > 1$, as well as for $Q = 1$ and $P < 1$. The amplitude and period of the cycles increase with increasing difference between Q and P.

An continuously stable strategy (CSS) exists at the value of Q and P at which the equilibrium resource density reaches a minimum. The CSSs for Q and P are indicated with dashed vertical lines in figure 2.1 and both are within the stable region of parameter space. From this point onward we refer to the CSS-values of Q and P as $\bar{Q}$ and $\bar{P}$, respectively. We confirmed convergence stability of $\bar{Q}$ and $\bar{P}$ within the parameter range of population cycles by explicitly assessing the growth rate of mutant phenotypes in the cyclic attractor of the resident phenotype. For all values of Q and P, the mutant with a trait value closer to the CSS successfully invades and replaces the resident population. The evolutionary isoclines of $\bar{Q}$ as a function of P as well as $\bar{P}$ as a function of Q are shown in the $Q - P$-parameter space in

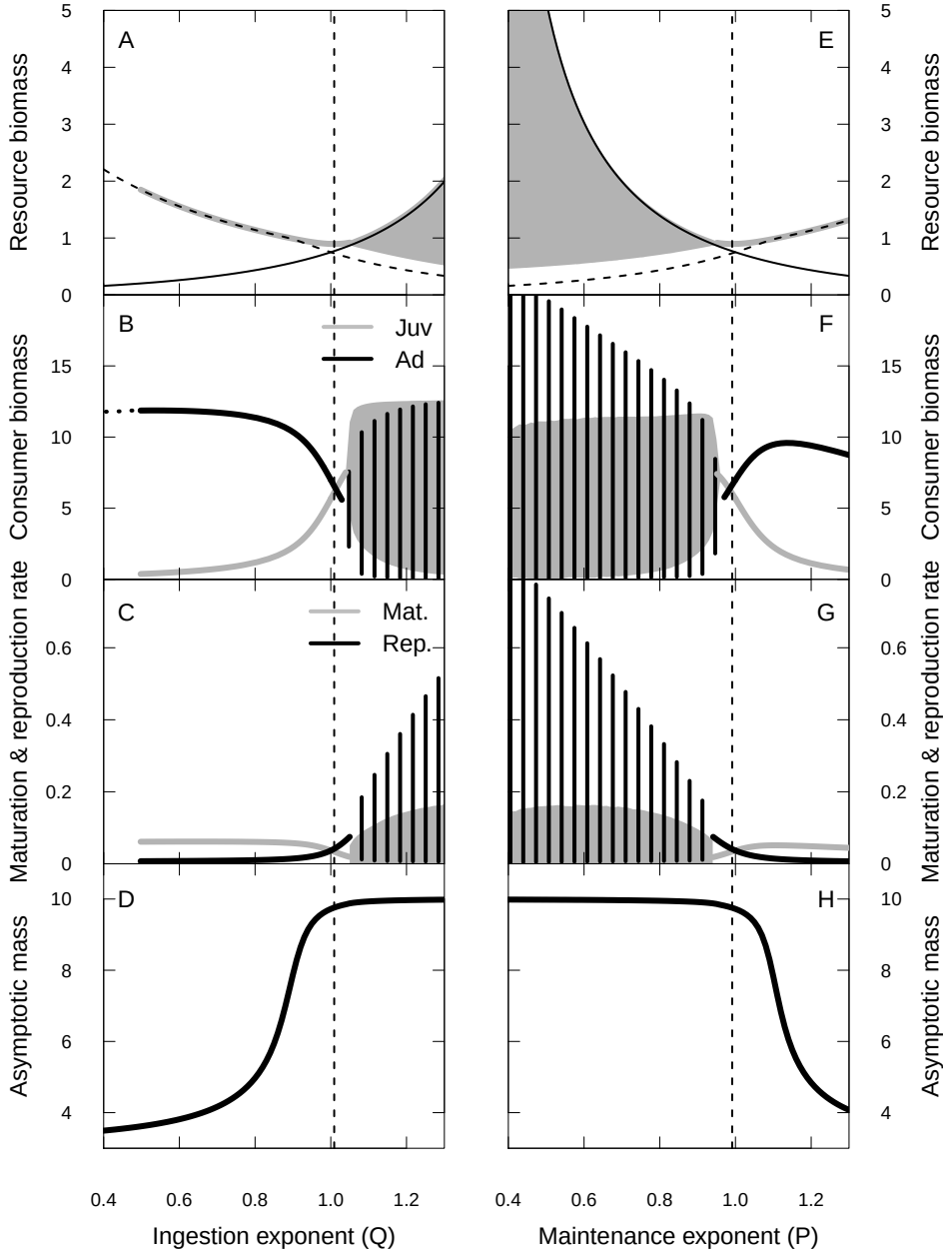

FIGURE 2.1 – Model dynamics as a function of the maximum ingestion scaling exponent Q (left with $P = 1$) and the maintenance rate scaling exponent P (right with $Q = 1$). Thick lines indicate stable model equilibria, while the solid-filled and dashed areas show the range and extent of population cycles. A,E: resource biomass (gray thick lines and shading) and the maintenance resource density (MRD) for the smallest (solid black lines) and largest (dashed black lines) individuals in the population. B,F: adults and juvenile biomass. C,G: total population reproduction rate and maturation rates in biomass. D,H: body mass of largest individuals in the population (asymptotic body size). The vertical thick dashed lines show the position of the CSS of Q in panels A:D, and the CSS of P in E:H. All other parameters as in table 2.2.

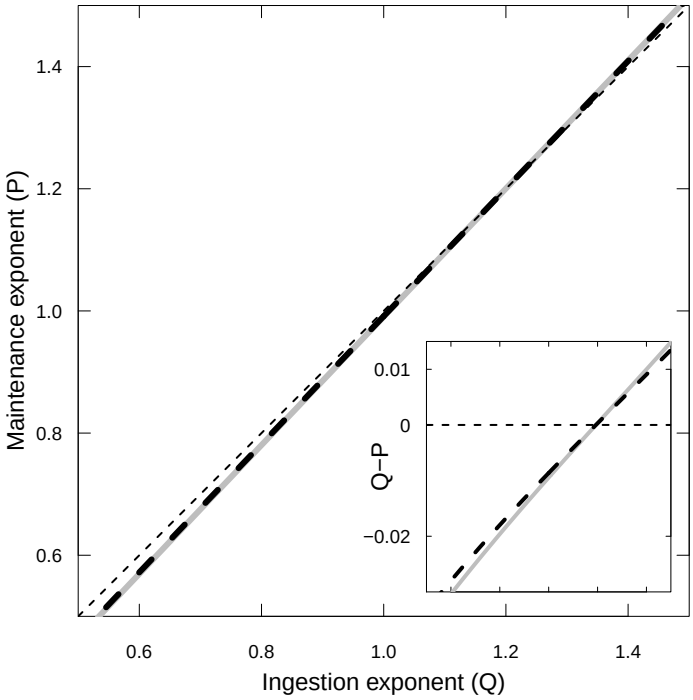

Figure 2.2 – Evolutionary isoclines, showing the value of the CSS of Q as a function of P (gray line), and the CSS of P as a function of Q (black dashed line) in the $Q-P$-plane. The thin dashed line represents the line where $Q = P$. The inset shows the difference between each of the two evolutionary isoclines and the line $Q = P$, as a function of Q (x-axis range identical to main figure). Isoclines cross exactly when this difference is zero (indicated by thin dashed line). All other parameters as in table 2.2.

figure 2.2. The isoclines appear to be on top of each other, but closer inspection reveals that they cross at $\bar{Q} = \bar{P}$ (inset figure 2.2). The small difference between the isoclines means that the CSS-value of one scaling exponent is approximately equal to the value of the other, non-evolving, scaling exponent. Therefore, evolutionary change in only one scaling exponent leads to approximately the same value of the other scaling exponent. Moreover, the evolutionary isoclines cross at zero difference, which implies that the CSS of both Q and P has the property that $\bar{Q} = \bar{P}$. For the default parameters (table 2.2), the common CSS-value is $\bar{Q} = \bar{P} \approx 1.19$. For this CSS-point the MRD does not change with body size, while the MBP increases with size, since $\bar{Q} = \bar{P} > 1.0$. Per unit biomass, larger individuals produce more new biomass than smaller individuals and the population-level biomass reproduction rate exceeds the population-level biomass maturation rate. In appendix 2.A we show that the convergence of the two exponents to the same value is independent of the assumption $s_r = s_j$, while the scaling of the MBP with body mass in the CSS-point is

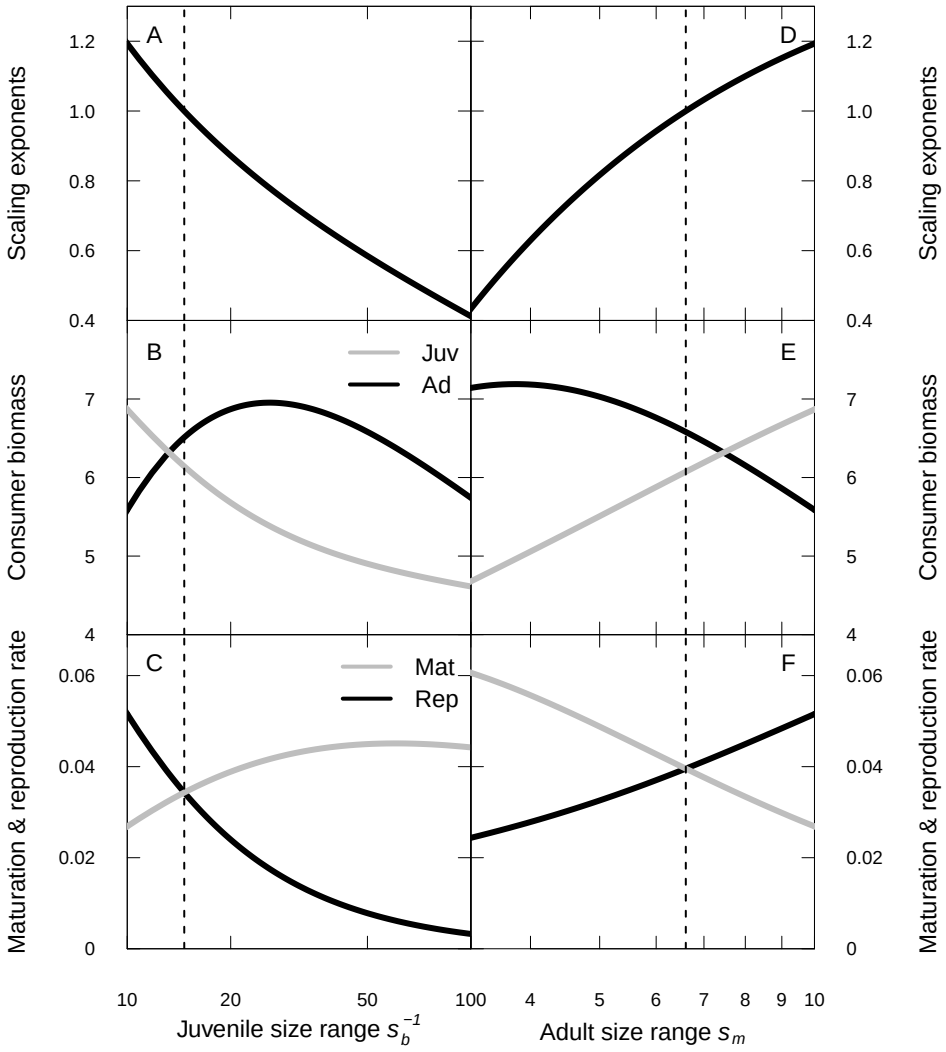

Figure 2.3 – CSS-values of scaling exponents of maximum ingestion rate Q and maintenance rate P (A,D: black line), as a function of the juvenile size range, parameterized by s_b^{-1} (A-C) and the adult size range, parameterized by s_m (D-F). A,D: common scaling exponent of maximum ingestion and maintenance rate. B,E: adult and juvenile consumer biomass. C,F: population-level reproduction and maturation rates in biomass. The vertical dashed lines indicated the value of s_b^{-1} (A-C) and s_m (D-F) where $\bar{Q} = \bar{P} = 1$.

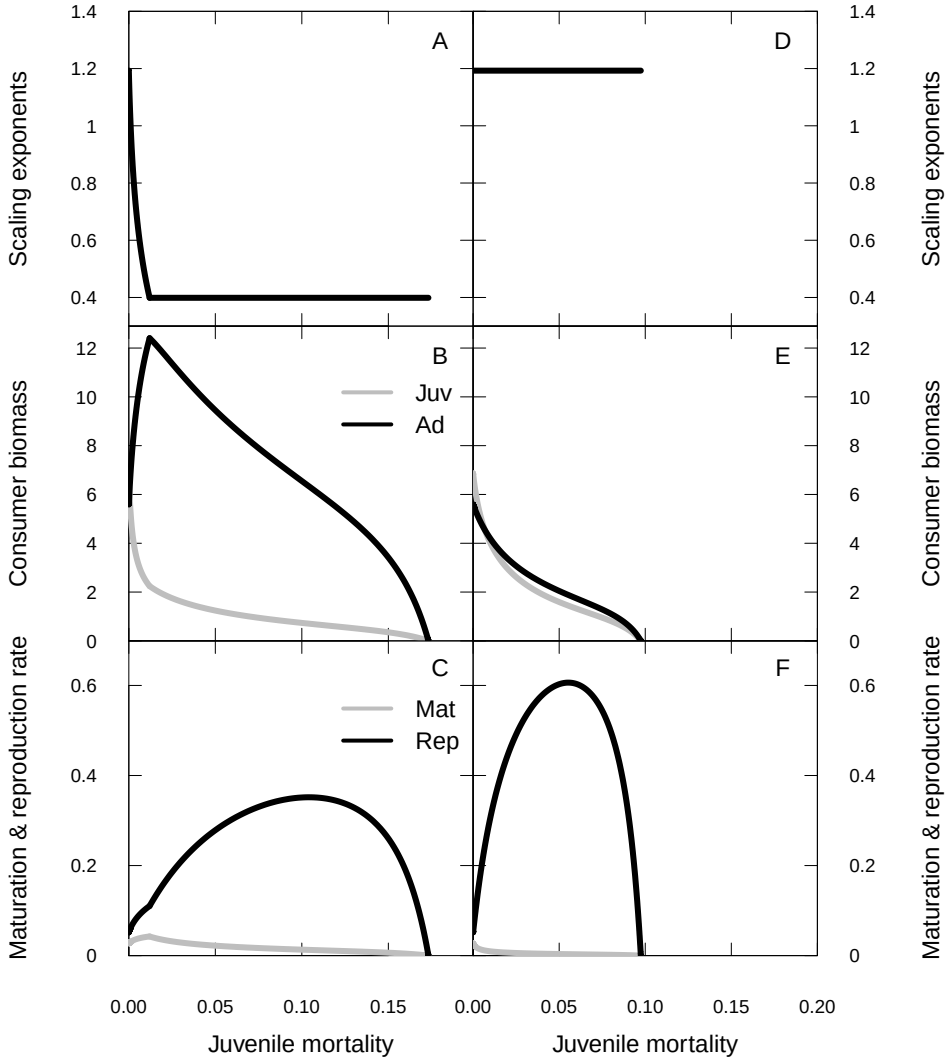

Figure 2.4 – Equilibria as a function of increasing mortality for juveniles (μ_j), for evolving (A-C) and non-evolving scaling exponents (D-F). A,D: common scaling exponent of maximum ingestion and maintenance rate. B,E: adult and juvenile consumer biomass. C,F: population-level reproduction and maturation rates in biomass. Default parameters as in table 2.2 where $\bar{Q} = \bar{P} = 1.193$ at $\mu_j = 0.0$.

dependent on the reference size s_r. Increasing the value of s_r leads to a decrease of $\bar{Q} = \bar{P}$.

The evolutionary convergence of the scaling exponents to a common CSS-value is robust against changes in the size at birth and the maximum body size. However, the value of the evolutionary endpoint is influenced by these size parameters. In general, increasing the size range of a life stage changes $\bar{Q}$ and $\bar{P}$ such that the MBP of this life stage increases. Figure 2.3 shows the effect of changing size at birth and maximum size on $\bar{Q}$ and $\bar{P}$. A decrease in s_b and hence an increase in the juvenile size-range decreases the common CSS-scaling exponent, which increases the MBP for small individuals. This leads to an increase in maturation rate and a decrease in reproduction rate (figure 2.3C). Biomass accumulates in the adult life stage and the juvenile/adult biomass ratio decreases. Alternatively, a larger adult size range increases the common value of $\bar{Q}$ and $\bar{P}$ (figure 2.3D). As a consequence, the reproduction rate increases, the maturation rate decreases and the consumer population becomes dominated by juveniles (figure 2.3E,F). Their is a combination of s_b and s_m values for which $\bar{Q} = \bar{P} = 1$. This size ratio is indicated with vertical dashed lines in figure 2.3. Only for this combination of juvenile and adult size ranges, does the model predict the MBP to be independent of body size.

The evolutionary response to increasing juvenile and adult mortality is shown in figure 2.4 and appendix figure 2.C1. This evolutionary response is compared with the response to increasing mortality when the scaling exponents do not evolve (figure 2.4D-E). In case of increased juvenile mortality and non-evolving scaling exponents, $Q = P > 1$ and this causes a larger MBP for adults compared to juveniles. This can be inferred from the population level reproduction rate being larger than the population level maturation rate (figure 2.4F). Increasing juvenile mortality initially increases reproduction rate due to increased resource availability (not shown), while maturation rate immediately decreases for non-evolving scaling exponents. In case of evolving scaling exponents, $\bar{Q}$ and $\bar{P}$ are again equal. However, additional juvenile mortality does change the common CSS-value. Increasing juvenile mortality (μ_j; figure 2.4) decreases $\bar{Q} = \bar{P}$ such that the increased loss rate of juvenile biomass is compensated for by an increased juvenile MBP. This compensatory response does not change the result that $\bar{Q} = \bar{P}$. Therefore, juveniles also suffer from increased maintenance costs due to a decrease in P. The decrease in $\bar{Q} = \bar{P}$ leads to an increase in adult biomass and even total consumer population biomass, until the exponents hit the lower constraint of 0.4. This initial increase comes about through an increase in maturation rates (figure 2.4C), while for a constant Q and P the maturation rate never increases and there is no increase in stage-specific biomass with increasing mortality (figure 2.4E,F). Further increases in mortality lead to a decrease of consumer biomass until the consumer goes extinct at juvenile mortality values that are substantially higher compared to those in

the absence of an evolutionary response. The response to increased adult mortality (μ_a) is comparable but leads to higher rather than lower values of $\bar{Q}$ and $\bar{P}$ and an increase in juvenile biomass through an increase in reproduction rate (see appendix figure 2.C1). This increase also only occurs for evolving scaling exponents. Similar to increased juvenile mortality, the consumer goes extinct at higher adult mortality rates when the scaling exponents evolve compared to non-evolving exponents (figure 2.C1).

2.4 – Discussion

Recent studies show considerable variation in the intraspecific scaling of maintenance metabolism with body size and relate this variation to ecological and environmental factors such as, among others, temperature, lifestyle, predation, body shape and activity level (Caruso et al. 2010; Glazier 2005, 2010; Glazier et al. 2011, 2015; Hirst et al. 2014; Killen et al. 2010; Ohlberger et al. 2012*b*, 2007). Metabolic rates affect competitive ability. Therefore, changes in competitive ability during ontogeny can arise through changes in the scaling of metabolic rate with body mass. The population and community effects of such size-dependent changes in competition are well documented. Here we report the first results on the evolutionary dynamics of the scaling of competitive ability with body size. In case of a trade-off in the energetics between small and large bodied individuals (newborn or juveniles versus adults), the scaling exponents of maximum ingestion and maintenance evolve to minimize the competitive asymmetry within the population. This is achieved when maintenance and ingestion scale in the same way with body size. Only in this case all differently-sized individuals are equal with respect to the resource density they require to cover their maintenance costs. We show that this result is robust against changes in the juvenile and adult size ranges (figure 2.3), size-dependent mortality (figure 2.4 and appendix figure 2.C1) and the reference size on which the scaling exponents are parameterized (appendix figure 2.A1).

The evolutionary prediction of equal scaling exponents of maintenance and maximum ingestion is at odds with the existing theories about ontogenetic growth. These theories assume an isometric increase of maintenance costs ($P = 1$) and a sublinear allometry of maximum ingestion rates ($Q = 3/4$ or $Q = 2/3$ Hou et al. 2008; Kooijman 2010; Moses et al. 2008; Van der Meer 2006; West et al. 2001, 2004). Such a combination of scaling exponents leads to a decrease in competitive ability over ontogeny, as measured by the maintenance resource density. We show that this results in negative selection on the maintenance exponent and positive selection on the maximum ingestion exponent. Also, our results show that when either Q or P is fixed, the other exponent still evolves to a value close to the evolutionarily constrained scaling exponent. Therefore, in this model there can only be a difference between both exponents

when they are both constrained and non-evolvable. Selective change in one or both exponents will eventually bring them together.

It is difficult to assess experimentally whether the scaling of maintenance rate is different from that of ingestion. One reason is that the exact maintenance costs are often hard to quantify. Measures like resting or basal metabolic rate are used frequently, but even when organisms are not feeding they can still invest in growth or reproduction. In which case the measured metabolic rate still includes overhead costs for these investments (Kooijman 1986; McCauley et al. 1990). Even if measurements of metabolic rate of non-feedings individuals would provide a reliable estimate of their maintenance costs, the resulting scaling exponents often show considerable variation (Glazier 2005). Likewise, the scaling of ingestion rate with body size or volume also varies considerably (Maino and Kearney 2015). DEB theory assumes that ingestion is a surface related process and scales with a two-thirds power of (structural) volume (Kearney and White 2012). This appears to be true for non-volant mammals, in which the small intestinal surface area scales with body mass$^{2/3}$. However, the pooled mass exponent for both non-volant mammals and birds is 0.73 and for birds alone it is even higher (Kearney and White 2012). For insects the surface-area scaling of ingestion describes the central tendency when averaged across several species, but for 8 out of the 38 species (21%) tested by Maino and Kearney (2015), the scaling exponent was significantly different from two-thirds. Due to the variation in scalings of both maintenance and ingestion rates a comparison between the two can only be informative when measurements are performed under identical conditions and for the same species or even the same population. This considerably limits the amount of information available to compare scalings of ingestion with those for maintenance rate.

A well studied case is that of *Daphnia* sp., in which the dependence of ingestion and maintenance metabolism was reviewed by McCauley et al. (1990) and Gurney et al. (1990). Maintenance rates of *Daphnia* sp. increased superlinear with body mass (> 1) due to contributions to carapace formation (McCauley et al. 1990). Ingestion rates were best described by separate functions for juveniles and adults (McCauley et al. 1990), but the overal scaling exponent was approximately 0.73. Models of ontogenetic growth in which maintenance costs increase faster with body mass than ingestion rates lead to decreasing growth rates with increasing size. Such a pattern often performs well in describing observed growth trajectories (Peters 1983; Ricklefs 2003). Equal scaling exponents would lead to an exponential growth pattern, which are less often observed (Kooijman 2010). In conclusion, the data from Daphnia and most growth patterns show that the maintenance rate scaling exceeds the ingestion rate scaling. This contradicts the evolutionary prediction of equal scaling exponents.

Another way to assess the scaling of maintenance and ingestion rates is to study the scaling of the MRD with body size directly from experiments that measure individual growth at different food levels and from this derive the food density where growth is zero (Gliwicz 1990; Kreutzer and Lampert 1999). Several studies indicate that the MRD is an increasing function of size, leading to a competitive advantages of small individuals (Aljetlawi and Leonardsson 2002; Byström and Andersson 2005; Byström et al. 2006; Hjelm and Persson 2001; Jansen et al. 2003; Lefébure et al. 2014). Aljetlawi and Leonardsson (2002) show that the MRD increases with body size in the amphipod *Monoporeia affinis* and that this increase is attributable to an decrease in handling time (which in Holling's functional response is the inverse of maximum ingestion) with mass$^{0.43}$, while resting metabolic rates increases isometrically with size. Consequently, juveniles are competitively superior to adults, which provides an explanation for the often observed fluctuating population dynamics of this species (Aljetlawi and Leonardsson 2002). The often observed increase of the MRD with body size is at odds with equal scaling exponents of maintenance and ingestion.

As shown in figure 2.4E and appendix figure 2.C1E, equal scaling exponents prevent the occurrence of biomass overcompensation. This is the increase in stage-specific biomass with increasing mortality (De Roos et al. 2007). Schröder et al. (2014) conclude that biomass overcompensation is likely to be commmon in natural systems and especially leads to increases in juvenile biomass. Overcompensation in juvenile biomass is indicative of an energetic bottleneck in the adult life stage. A higher scaling of maintenance metabolism compared to the scaling of ingestion could lead to such an energetic bottleneck for adults. A community consequence of biomass overcompensation is the emergent Allee effect, in which a size-specific predator changes the size distribution of its prey to ensure its own persistence (De Roos et al. 2003*b*; Van Kooten et al. 2005). Emergent Allee effects have been found in freshwater fish stocks (Persson et al. 2007) and cannot occur without an energetic bottleneck in the prey population. The observed stable population dynamics for equal scaling exponents provides another indication that the true exponents of maintenance and ingestion differ. As shown in figure 2.1, equal scaling exponents lead to stable population dynamics. This contradicts laboratory and empirical observations of fluctuating population dynamics for *Daphnia* sp. (McCauley et al. 2008, 1999) and the suggestion that cyclic population dynamics are widespread in nature (Murdoch et al. 2002).

In summary, the detailed studies on the physiology and population dynamics of *Daphnia* sp, the observed increase in the MRD with body size in several fish and crustacean species and the observed population and community consequences of unequal scaling exponents all support the tenet that maintenance rates increase faster with body mass than ingestion rates. This is at odds with the evolutionary predictions derived in this paper. One simple explanation for this discrepancy could be that the

scaling exponents are constrained and hence cannot evolve. There is at least some evidence against this explanation. First of all, the range of observed intraspecific scaling exponents does suggest there is variation for selection to act on (Glazier 2005; Moses et al. 2008). This variation has been related to lifestyle, activity, growth form, temperature and predation (Glazier 2005, 2006; Killen et al. 2010; Kiørboe and Hirst 2014; Ohlberger et al. 2012*b*, 2007). For example, White et al. (2011) experimentally showed that metabolic rate scales with mass$^{0.5}$ for colonies of a bryozoan species, while other colonial marine invertebrates have scaling exponents of 0.75, 1 or 1.125 (Hughes and Huges 1986; Nakaya et al. 2003). These different scaling exponents are explained by the differences in growth forms of the colonies (White et al. 2011). Two-dimensional growth at the colony edge leads to exponents around 0.5, while growth forms that deviate from circular lead to higher exponents (White et al. 2011). Also on the individual level, body shape changes can influence the intraspecific scaling of metabolic rates. As shown by Hirst et al. (2014) growth in 3 dimensions (isomorphic growth) is related to low scaling exponents, while one dimensional growth (elongation) relates to exponents around one. These findings are in favor of theories that assume metabolic scaling to be determined by transport of materials across surfaces and indicate that changes in growth form can influence the scaling of resource supply rates. Selection would hence be able to change the scaling of maximum ingestion with body size by altering the dimension of ontogenetic growth.

Secondly, the possibility that the existing variation in the scaling of metabolic rate with body size is an evolutionary adaptive and phenotypically plastic response, is discussed by Ohlberger et al. (2012*b*). These authors show that in one pair of related coregonids (*Coregonus albula* and *C. fontanae*), which live in cold environments, the scaling exponent of metabolic rate with body mass decreases linearly with temperature, while in a pair of related cyprinids (*Abramis brama* and *Rutilus rutilus*), which live in warmer waters, the body-mass scaling of metabolic rate is independent of temperature. This indicates that the response of the body-mass scaling of metabolism to temperature differs between species or taxa and can be dependent on their environment or evolutionary history (Ohlberger et al. 2012*b*). The hypothesis that evolutionary adaptions to different environments can lead to differences in scaling exponents is further illustrated by Glazier et al. (2011). These authors show that the scaling of resting metabolic rate in the amphipod *Gammarus minus* depends on the presence of fish predators. Individuals from three populations that naturally co-occur with the predatory fish *Cottus cognatus* have lower scaling exponents than individuals from two populations in which these predators are absent. The lower scaling exponents for the individuals from the predatory lakes resulted in a higher metabolic rates for small individuals and a lower metabolic rate for large individuals. Furthermore, Glazier et al. (2011) show by using field enclosures that juvenile growth

is increased and adult growth is reduced in individuals from the fish-exposed populations. This resulted in faster growth towards lower asymptotic sizes. The results of Glazier et al. (2011) correspond to our evolutionary predictions in case of increasing juvenile mortality. This lowers the CSS of the common scaling exponent of maintenance and maximum ingestion, in order to increase the mass-specific biomass production (growth) of juveniles. The increase in mass-specific production of juveniles occurs at an expense of the mass-specific production of adults. This decreases adult growth, resulting in a decrease in asymptotic body size.

More complex ecological scenarios or life histories can possibly lead to different predictions about the evolution of the scaling exponents of metabolism. The current analysis shows that the evolutionary convergence of the body-mass scaling exponents of maintenance metabolic rate and maximum ingestion rate towards the same value is robust against changes in many of the model parameters. However, it remains to be studied to which extent this result depends on the current net-production allocation scheme or the consideration of a single, shared resource. Also, increased ecological complexity by incorporating additional ecological interactions are likely to affect the predictions. For example, complexity such as ontogenetic diet shifts, prey/predator size ratios and interference competition have been shown to reduce the size-dependency of the MRD, and in this way counteract the negative competitive effect of small individuals on the large conspecifics. For example, Aljetlawi and Leonardsson (2002) show that interference competition of large *M. affinis* increases the MRD of the smaller size-classes. Also ontogenetic diet shifts can reduce the negative effects of competition for large individuals. As observed in many fish species, the attack rate of zooplankton is a humped shaped function of body size, as foraging capacities become hindered by large size differences between predators and prey (Byström and Andersson 2005; Hjelm and Persson 2001). This often coincides with the size threshold at which individuals switch to a second resource, such as benthic macroinvertebrates or other fish species. Indeed, Byström and Andersson (2005) show that the increase of the MRD for Arctic char *Salvelinus alpinus* was substantially reduced when using macroinvertebrates as prey, instead of zooplankton. Also, Jansen et al. (2003) demonstrate that the decrease in attack rate of Arctic char on zooplankton occurs at a larger size when large zooplankton prey are used and that this substantially reduces the increase in MRD with body size. Future research should point out how the evolution of size-scaling exponents depend on additional ecological complexity, such as ontogenetic diet shifts or interference competition.

Furthermore, we show that the common value of the maximum ingestion and maintenance scaling exponents depends on the mortality rates and the size-ranges of the juvenile and adult life stages (figure 2.3, 2.4 and 2.C1). Either an increase in the juvenile size-range (for species with a lower size at birth) or a high juvenile mortality

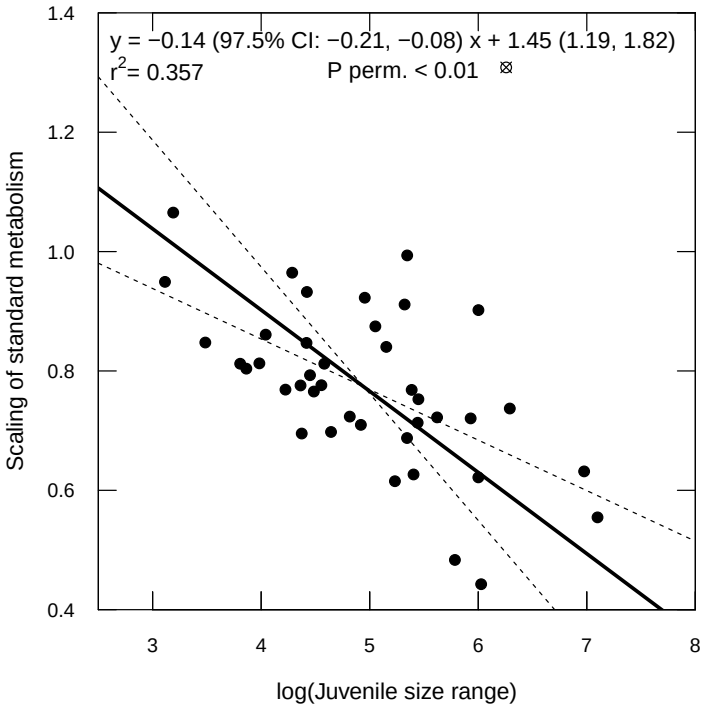

Figure 2.5 – The scaling of standard or routine metabolism with body size of 41 teleost fish species, versus the ratio of length at maturation and egg diameter, as a measure for the juvenile size-range. Data on scaling exponents are from Killen et al. (2010). See appendix 2.B for a detailed description of data collection and analysis. The lines show a RMA regression with 97.5% confidence intervals. The point indicated by the open circle with the cross is the eel *Anguilla anguilla*, which was not part of the regression equation (see appendix 2.B).

rate favor selection towards increased juvenile growth rates. Similarly, an increase in the adult size-range (for species with a higher maximum size) or a high adult mortality rate favor selection towards increased post-maturation growth and reproduction rates. On the basis of this work we therefore predict low scaling exponents for species that have a large size at maturation compared to size at birth or suffer from high juvenile mortality. Alternatively, species with a limited juvenile size-range or low juvenile mortality rates are expected to have higher scaling exponents for maintenance and ingestion, even so for species with high adult mortality or substantial opportunity for post-maturation growth. The quantitative predictions for the scaling exponents of maintenance and ingestion very much depend on these size and mortality parameters, but the qualitative trends remain unchanged.

We tested the prediction about the scaling of metabolism in relation to the juvenile size range by using data on scaling exponents of standard or routine metabolic rate for teleost fish as published by Killen et al. (2010) and Clarke and Johnston (1999) and combining these with estimates of size at maturation and size at birth. We obtained estimates for these size parameters for 41 of the 89 species in the original dataset of Killen et al. (2010). Instead of weight estimates we used length at maturation (l_{mat}) and egg diameter (l_{egg}), since these are more readily available for fish. In figure 2.5 the temperature-corrected scaling exponent of standard metabolism is plotted against the logarithm of l_{mat}/l_{egg}. The regression line in figure 2.5 results from a Ranged Major Axis model (Legendre 2014). In agreement with our prediction that the common scaling exponent of ingestion and maintenance rate decreases with an increase in the juvenile size range, figure 2.5 indeed shows a significant negative relationship between the scaling exponent of standard metabolism and the juvenile size-range, despite considerable variation in metabolic scaling exponents, egg diameters and maturation sizes (Bagenal 1971; Clarke and Johnston 1999; Kamler 2005; Killen et al. 2010). The data and references are available in appendix table 2.B1 and details on data collection and statistics are described in appendix 2.B.

In this study we ignore the proximate causes that lead to the allometric scaling of maintenance metabolism and ingestion and instead focus on the ultimate, evolutionary causes that are shaped by how individuals interact with each other through their interaction with a shared environment. Such interactions ultimately determine fitness and drive evolutionary change (Metz et al. 1992). Although this model considers a simplified individual energy budget and includes only the most simple environmental feedback, it provides a powerful and robust null model against which to evaluate evolutionary considerations regarding the intraspecific scaling of ingestion and maintenance with body size. The model predictions paradoxically contrast with a substantial amount of empirical findings, both observational and experimental. Further study should focus on the consequences of more complex ecological scenarios, as well as more complex life histories, for evolutionary dynamics of asymmetric, intraspecific competition.

Acknowledgments

This research was supported by funding from the European Research Council under the European Union's Seventh Framework Programme (FP/2007-2013) / ERC Grant Agreement No. 322814. Lennart Persson and Romain Richard provided useful comments that considerably improved the manuscript.

Appendix 2.A Supplementary figure

We assume a juvenile-adult trade-off in both maximum ingestion rate and maintenance rate. This trade-off is implemented by parameterizing the power functions that describe these rates, at the size at maturation. When another reference size than the size at maturation is used to fix these power functions, both exponents still evolve towards a common value. This CSS-value increases with decreasing reference size, see figure 2.A1

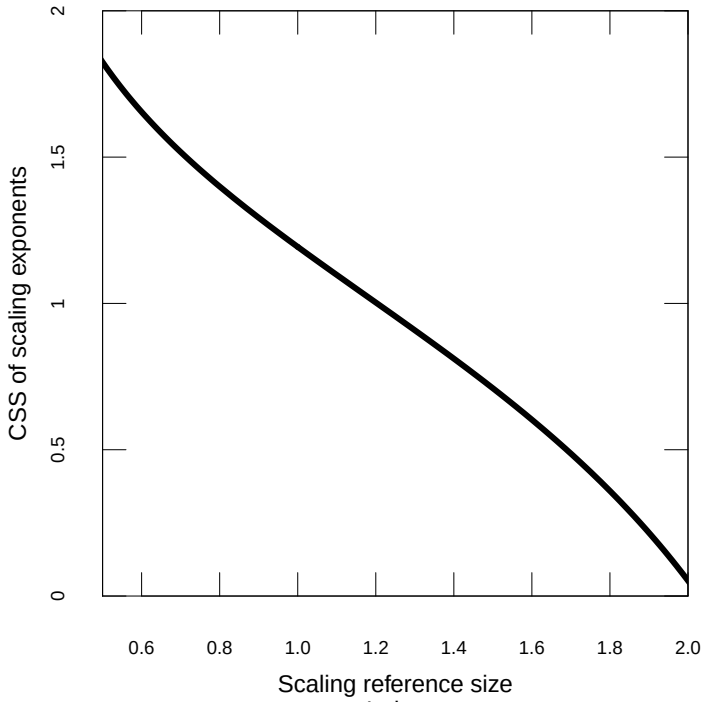

Figure 2.A1 – Value of the evolutionary equilibrium (CSS) of the common scaling exponent of maximum ingestion and maintenance rate, as a function of the scaling reference size s_r. All other parameters as in table 2.2.

Appendix 2.B Data collection and analysis

Data collection

Data on the relationship between metabolic rate and body mass were taken from the supporting information of Killen et al. (2010). This dataset provides estimates on metabolic scaling exponents (b) and metabolic activity level (L), defined as "the mass-specific metabolic rate estimated at the body mass corresponding to the midpoint of the allometric relationship" (Killen et al. 2010) for 89 species of Teleost fish. The data is an extension of the data provided by Clarke and Johnston (1999) and selection criteria handled by both Killen et al. (2010) and Clarke and Johnston (1999) were aimed at selecting rates of standard or routine metabolism. Only data on resting, post-larval, fasted animals measured in absence of additional stressors and after a 24h acclimation period were accepted (Killen et al. 2010). Additionally, the temperature (T) at which metabolism was measured should be within the natural temperature range of the species and the metabolism should be measured over a suitable body-mass range (see Clarke and Johnston 1999 and Killen et al. 2010 for a more detailed description of acceptance criteria).

To test the hypothesis that the scaling of metabolic rate changes with the ratio between size at birth and size at maturation we collected data on egg diameter (l_{egg}) and length at maturation (l_{mat}) for the species in the dataset of Killen et al. (2010). Length instead of mass estimates were used since the former are more readily available for fish. Furthermore, any pattern in the length ratios will remain intact after a non-linear transformation to mass ratios. Data collection was carried out at a species-specific level and the estimates for l_{mat} and l_{egg} are generally not from the same source, nor is any of the two directly derived from populations or individuals that were used for the metabolic rates measurements. There is considerable variation in both size at maturation and egg size between individuals of the same population, between different populations of the same species and with size and age of the parents (Bagenal 1971; Bøhn et al. 2004; Bonislawska et al. 2001; Kamler 2005; Wallace and Aasjord 1984). This variation could not be controlled for and is taken for granted since estimates performed on the same individuals for our variables of interest (l_{egg}, l_{mat} and b) were not available.

Various sources report different estimates of l_{egg} and l_{mat} for the same species and these data were averaged to arrive at a species-specific prediction. Main sources for maturation size estimates were Winemiller and Rose (1992), King and McFarlane (2003) and Fishbase (Froese and Pauly 2016). Fishbase estimates were collected using R (R Core Team 2015) with the package 'rfishbase' (Boettiger et al. 2016, 2012). Single estimates for l_{mat} were preferred over range estimates and the latter were only used when both minimum and maximum values were reported. Estimates of l_{egg} were

mainly derived from Winemiller and Rose (1992), King and McFarlane (2003) and Russel (1976). Additional searches for egg size were performed for species if size at maturation estimates were provided in the sources mentioned above. This resulted in a total of 41 species with estimates of l_{egg}, l_{mat} and b. All data and data source are reported in table 2.B1.

Data analysis

Killen et al. (2010) show an effect of the temperature (T) at which the metabolic measurements where performed on both the scaling of metabolism with body size (b) and on the metabolic level (L). Furthermore, the authors show an effect of $\log(L)$ on b. To correct for these dependencies in our analysis we calculate the effect of T on the $\log(L)$ for the original 89 species described in Killen et al. (2010). This analysis is identical to the one described in the figure S1 of the supporting information of Killen et al. (2010) and gives an ordinary least squares (OLS) regression of $\log(L) = 0.0653T + 3.17$ (slope $P < 0.0001$ and $R^2 = 0.510$). We used the residuals of the regression of $\log(L)$ against T relative to the prediction for $\log(L)$ at $T = 15°C$ to calculate temperature-corrected estimates of $\log(L)$. These temperature-corrected values are referred to as $\log(L_{Tcorr})$. We related $\log(L_{Tcorr})$ to the scaling exponents of metabolic rate of the original dataset of Killen et al. (2010). Contrary to the values of L the temperature-corrected values do not show a clear relationship with b (slope $= -0.0300$, $P = 0.176$, $R^2 = 0.0212$), indicating that the original effect of $\log(L)$ on b as reported by Killen et al. (2010) was mediated by temperature and not through an effect of $\log(L)$ directly. Due to the lack of a clear correspondence between the temperature-corrected values of $\log(L)$ on b we refrained from correcting estimates of b to the metabolic level L. Instead, we only controlled for a direct effect of T on b. This was done by recalculating the OLS regression between b and T as reported in figure S1b of Killen et al. (2010) and using the residuals of this regression equation ($b = -0.005872T + 0.875878$, slope $P < 0.0001$, $R^2 = 0.198$) relative to the predicted scaling exponent at $15°C$. These temperature-corrected values were calculated with the full dataset as reported by Killen et al. (2010) and used to test the hypothesis that the scaling of maintenance metabolism is negatively related with the ratio between size at maturation and size at birth for species for which these latter estimates were available (see table 2.B1).

We used ranged major axis (RMA) regression to calculate the correlation between $\log(l_{mat}/l_{egg})$ and the temperature-corrected scaling exponent b_{Tcorr} (main text figure 2.5). Since RMA regression is sensitive to the presence of outliers (Legendre 2014). Cook's distance was calculated from an OLS regression of b_{Tcorr} on $\log(l_{mat}/l_{egg})$. The estimates for the eel (*Anguilla anguilla*) had a Cook's distance of 0.697, which was 6.2 times the value of the second highest Cook's distance. Therefore, we de-

cided to exclude the eel from further analysis, since it has a disproportionally large effect on the estimates of the OLS regression. The RMA regression line relating the temperature-corrected scaling exponent of metabolism to the juvenile size-range is: $b_{Tcorr} = -0.14 \log(l_{mat}/l_{egg}) + 1.45$, with $n = 40$, $R^2 = 0.357$ and a one-tailed permutation test of the slope of $P < 0.01$ (main text figure 2.5). This negative correlation supports the evolutionary prediction that an increased juvenile size-range through either a smaller size at birth (measured as egg diameter) or an larger size at maturation should result in lower scaling exponents of metabolism with body size.

TABLE 2.B1 – Dataset used for figure 2.5 (main text)

Species	l_{egg} (mm)	Source	l_{mat} (mm)	Source	l_{mat}/l_{egg}	b	T(°C)	L (mg kg^{-1} h^{-1})	log(L_{Tcorr})	b_{Tcorr}
Alosa sapidissima	3.17		433		137	0.695	17.5	111.22	4.55	0.71
Ameiurus nebulosus	3.00	1,2	218	1	73	0.994	10	34.02	3.85	0.96
Anguilla anguilla	1.15	6	600	2	522	1.291	18	19.83	2.79	1.31
Bathylagus antarcticus	2.10	9	100	2	48	0.889	0.5	20.35	3.96	0.8
Brevoortia tyrannus	1.62	1,5,7	253	1,2	156	0.816	25	328.58	5.14	0.87
Catostomus commersonii	3.13	1,2	260	1	83	0.903	20	62.86	3.81	0.93
Chaenocephalus aceratus	4.13	2	429	2	104	0.78	1	26.98	4.21	0.7
Chelon labrosus	1.30	10	273	2	210	0.976	18	171.64	4.95	0.99
Coryphaena hippurus	1.43	2,7	593	2	414	0.384	25	192.52	4.61	0.44
Cyprinus carpio	1.72	1,2,6	297	1,2	173	0.781	25.1	86.29	3.8	0.84
Dorosoma cepedianum	0.87	1,2,5	282	1,2	325	0.454	20	105.38	4.33	0.48
Electrona antarctica	1.30	9	74	2	57	0.946	0.5	56.55	4.98	0.86
Eleginus gracilis	1.35	11	300	2	222	0.7	2.5	47.6	4.68	0.63
Euthynnus affinis	0.48	12	575	2	1211	0.496	25	337.86	5.17	0.55
Gadus macrocephalus	1.02	1,3	550	1,2,3	540	0.787	6.5	49.84	4.46	0.74
Gadus morhua	1.49	1,4,5,7,8	561	1,2	376	0.791	3	52.77	4.75	0.72
Gasterosteus aculeatus	1.67	1,2,6	38	1,2	23	1.008	5	168.78	5.78	0.95
Gymnocanthus tricuspis	2.00	13	90	2	45	0.909	-1.5	25.68	4.32	0.81
Hippoglossoides platessoides	2.41	4,8	298	2	124	0.794	3	16.3	3.58	0.72
Katsuwonus pelamis	1.03	1,7	414	1,2	404	0.563	25	269.1	4.94	0.62
Lepomis gibbosus	1.03	1,2	70	1	68	0.71	25	38.07	2.99	0.77
Lepomis macrochirus	1.30	1,2	102	1	78	0.717	25	34.11	2.88	0.78

Continues on next page

TABLE 2.B1 – *Continued from previous page*

Species	l_{egg} (mm)	Source	l_{mat} (mm)	Source	l_{mat}/l_{egg}	b	T(°C)	L (mg kg^{-1} h^{-1})	log(L_{Tcorr})	b_{Tcorr}
Limanda limanda	0.95	5,7,8	220	2	232	0.782	10	28.37	3.67	0.75
Mallotus villosus	1.00	1	142	2	142	0.864	25	114.2	4.08	0.92
Microstomus kitt	1.29	7,8	270	2	209	0.717	10	39.04	3.99	0.69
Mugil cephalus	0.83	7,8	333	2	404	0.855	23	177.57	4.66	0.9
Myoxocephalus scorpius	2.15	5,8	210	2	98	0.909	-1.5	43.6	4.85	0.81
Oncorhynchus mykiss	4.63	1,2,6	411	1	89	0.789	11	82.77	4.68	0.77
Oncorhynchus nerka	5.38	1,3	446	1,2,3	83	0.847	15	54.2	3.99	0.85
Oreochromis niloticus	3.60	5	193	2	54	0.754	25	45.8	3.17	0.81
Platichthys flesus	0.96	5,8	209	2	218	0.827	5	19.48	3.62	0.77
Pleuronectes platessa	3.03	4,5,8	288	2	95	0.782	14	63.16	4.21	0.78
Salmo trutta	5.01	2,6	163	2	33	0.877	10	72.4	4.61	0.85
Salvelinus alpinus alpinus	4.80	1,2,6	381	1,2	79	0.748	6	32.64	4.07	0.7
Salvelinus fontinalis	4.90	1,2	119	1	24	1.036	20	148.62	4.67	1.07
Sander vitreus	1.93	1,2	394	1	205	0.882	20	69.59	3.92	0.91
Sebastolobus alascanus	1.30	1,3	243	2,3	187	0.674	5	8.46	2.79	0.62
Theragra chalcogramma	1.40	3	387	2,3	276	0.778	5.5	67.53	4.83	0.72
Thunnus albacares	0.97	7,14	1033	2	1070	0.573	25	203.33	4.66	0.63
Trachurus trachurus	0.93	8	214	2	231	0.725	13	53.65	4.11	0.71
Zoarces americanus	3.50	15	299	2	86	0.834	8	70.46	4.71	0.79

[1] Killen et al. (2010) [2] Bagenal (1971) [3] King and McFarlane (2003) [4] ICES (2015) [5] Neuheimer et al. (2016) [6] Bonislawska et al. (2001) [7] Pauly and Pullin (1988) [8] Russel (1976) [9] Kock (1992) [10] Crosetti and Cordisco (2004) [11] Dunn and Matarese (1987) [12] Nissar et al. (2015) [13] `species-identification.org` [14] Margulies et al. (2007) [15] Steimle et al. (1999)

Appendix 2.C Supplementary figure

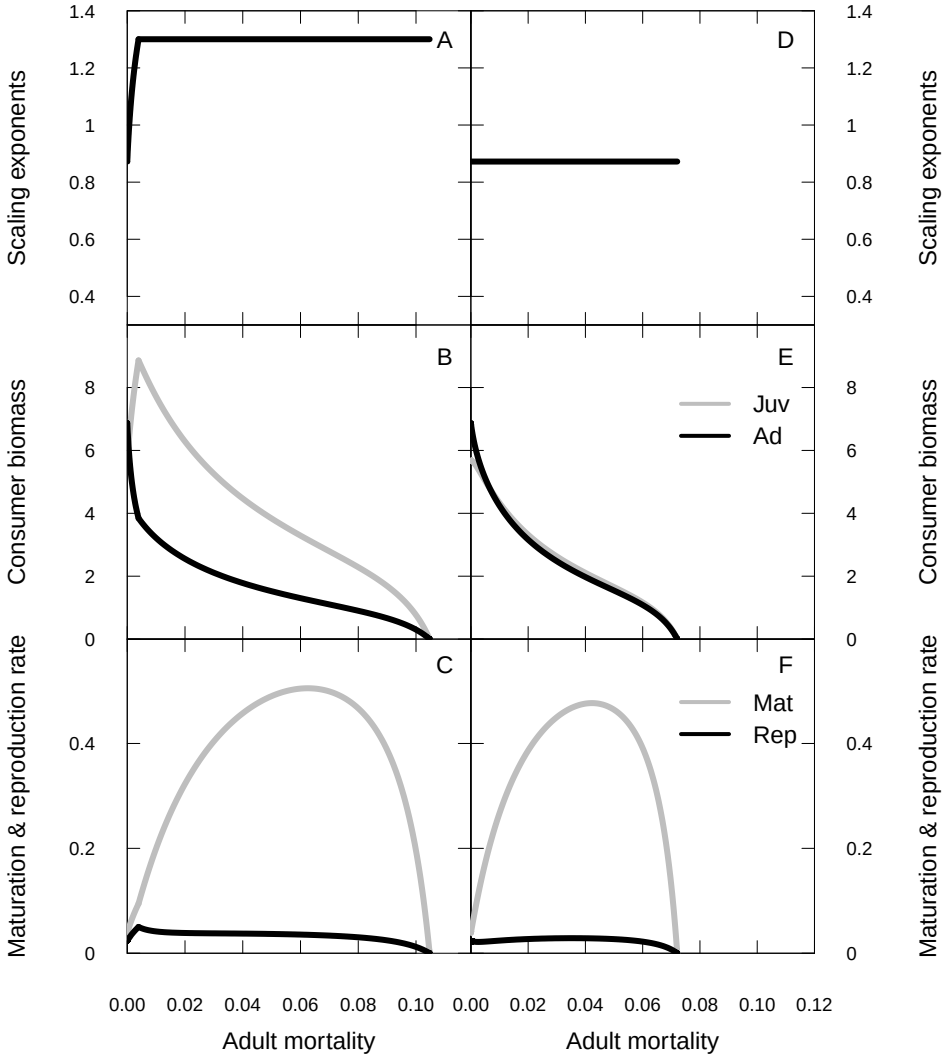

Figure 2.C1 – Equilibria as a function of increasing mortality for adults (μ_a), for evolving (A-C) and non-evolving scaling exponents (D-F). A,D: common scaling exponent of maximum ingestion and maintenance rate. B,E: adult and juvenile consumer biomass. C,F: population-level maturation and reproduction rates in biomass. Default parameters as in table 2.2, in addition to $s_b = 0.05$, for which $\bar{Q} = \bar{P} = 0.872$ at $\mu_a = 0.0$.